



Joint survey of the experimental high-resolution spectra of $\text{H}^{16}\text{O}^{37}\text{Cl}$ and $\text{H}^{16}\text{O}^{35}\text{Cl}$ with a reanalysis of the $2\nu_2$ band

Gábor Ecséri^a, Irén Simkó^a, Tibor Furtenbacher^b, Balázs Rácsai^a, Luciano Fusina^c, Gianfranco Di Lonardo^c, Kirk A. Peterson^d, Attila G. Császár^{a,b,*}

^a Institute of Chemistry, ELTE Eötvös Loránd University, H-1117 Budapest, Pázmány Péter sétány 1/A, Hungary

^b HUN-REN-ELTE Complex Chemical Systems Research Group, H-1518 Budapest 112, P.O. Box 32, Hungary

^c Dipartimento di Chimica Industriale 'Toso Montanari', Università di Bologna, Bologna, Italy

^d Department of Chemistry, Washington State University, Pullman, WA 99164, USA

ARTICLE INFO

Keywords:

High-resolution rovibrational spectroscopy

Spectroscopic data

$\text{H}^{16}\text{O}^{35}\text{Cl}$

$\text{H}^{16}\text{O}^{37}\text{Cl}$

MARVEL

Empirical energy levels

Spectrum assignment

ABSTRACT

The study starts with a detailed analysis of all the high-resolution rovibrational transitions measured for the minor hypochlorous acid isotopologue $\text{H}^{16}\text{O}^{37}\text{Cl}$, employing the MARVEL (Measured Active Rotational-Vibrational Energy Levels) procedure. The survey considers 16 sources, the wavenumber coverage of the transitions extends from the microwave to the visible region, corresponding to 13 vibrational parent states. Experimental transitions data from older (1994, 1996, and 2000) sources, not published explicitly in the original papers, are presented in here for the first time; the newly reported transitions represent about one third of all the transitions assigned for $\text{H}^{16}\text{O}^{37}\text{Cl}$. Then a minor update to the transitions and levels of $\text{H}^{16}\text{O}^{35}\text{Cl}$ published in *J. Mol. Spectrosc.* 384 (2022) 111561 is provided. Proper labelling and internal consistency of the transitions and the empirical rovibrational energies of $\text{H}^{16}\text{O}^{35}\text{Cl}$ and $\text{H}^{16}\text{O}^{37}\text{Cl}$ is enforced utilizing effective Hamiltonian (EH) and first-principles variational nuclear-motion computation results. An iteratively updated line list, based on empirical and EH rovibrational energy levels and first-principles intensities, is used to assign a significant number of new transitions in the $2\nu_2$ band ($2300\text{--}2800\text{ cm}^{-1}$) for both isotopologues. At the end, for $\text{H}^{16}\text{O}^{35}\text{Cl}/\text{H}^{16}\text{O}^{37}\text{Cl}$, from the total of 20 349/10 266 experimentally measured transitions considered, 20 119/10 124 could be validated, allowing the derivation of 5760/3933 empirical rovibrational energy levels with well-defined uncertainties. Improved parameters for an effective Hamiltonian corresponding to the $2\nu_2$ state are given. A comparison with data in the canonical spectroscopic line-by-line database HITRAN is also provided.

1. Introduction

In 2022 [1], some of the authors of this paper performed an analysis of rotationally-resolved spectra measured for the main hypochlorous acid isotopologue, $\text{H}^{16}\text{O}^{35}\text{Cl}$. Ref. [1] lists a number of reasons why it is important to study spectra of hypochlorous acid at high resolution; thus, they are not repeated here. It is only mentioned that HOCl is molecule #21 in the canonical line-by-line spectroscopic information system HITRAN [2,3], exemplifying the significance of HOCl for the modelling of planetary atmospheres.

Under natural abundance, the ratio of the ^{35}Cl and ^{37}Cl isotopes is approximately 3:1. Spectra of HOCl cannot be understood without the consideration of $\text{H}^{16}\text{O}^{37}\text{Cl}$; thus, almost without exception, papers dealing with the spectroscopy of $\text{H}^{16}\text{O}^{35}\text{Cl}$ contain measured data on $\text{H}^{16}\text{O}^{37}\text{Cl}$, as well. As a natural continuation of Ref. [1], this paper starts with our investigation of the high-resolution spectra and the underlying rovibrational energy level structure of the

$\text{H}^{16}\text{O}^{37}\text{Cl}$ isotopologue. Similar to Ref. [1], the MARVEL (Measured Active Rotational-Vibrational Energy Levels) technique [4–7], based on the theory of spectroscopic networks [8–10], is employed to obtain, following the validation of the available measured rovibrational transitions, empirical rovibrational energy levels with well-defined uncertainties. The present investigation can be characterized by several new features when compared to the MARVEL survey of the rovibrational spectra of $\text{H}^{16}\text{O}^{35}\text{Cl}$ [1]. First, the rovibrational energies determined are checked against effective Hamiltonian (EH) values, whenever both sets are available. This comparison is carried out for both isotopologues. Second, a detailed comparison of the empirical energy levels with those of first-principles variational nuclear-motion calculations is performed, helping to ensure the validity and the consistency of the rovibrational energy levels and labels of the two main HOCl isotopologues. Third, based on wave functions computed for a very large

* Corresponding author at: Institute of Chemistry, ELTE Eötvös Loránd University, H-1117 Budapest, Pázmány Péter sétány 1/A, Hungary.
E-mail address: attila.csaszar@ttk.elte.hu (A.G. Császár).

Table 1

Experimental sources used to construct the $\text{H}^{16}\text{O}^{37}\text{Cl}$ rovibrational spectroscopic network of this study. The data given include, for each source, the wavenumber ranges of the validated transitions, the number of actual (*A*), validated (*V*), and deleted (*D*) transitions, and selected uncertainty statistics, where *AIU* = average initial uncertainty and *AMR* = average MARVEL reproduction of the source's lines.

Source tag	Range/cm ⁻¹	A/V/D	AIU/cm ⁻¹	AMR/cm ⁻¹
84SiAnDaGe [16]	0.349–19.656	49/49/0	2.70×10^{-6}	3.52×10^{-8}
69LiLiMi [12]	0.978–0.978	1/1/0	1.67×10^{-6}	1.65×10^{-7}
98FIBiWaOr [25]	1.433–377.742	3191/3186/0	2.00×10^{-4}	2.59×10^{-5}
71MiScCa [13]	1.943–1.969	2/2/0	1.60×10^{-6}	1.47×10^{-7}
90CaLoFuTr [18]	30.306–208.974	792/792/0	2.00×10^{-4}	1.20×10^{-4}
95BeNaFuMo [21]	60.408–178.135	34/34/0	2.66×10^{-6}	4.14×10^{-8}
86LaOl [17]	685.058–1278.641	366/365/0	4.00×10^{-4}	6.26×10^{-4}
00AuKlFlPa [26]	1202.281–1270.757	181/101/0	1.30×10^{-4}	5.64×10^{-5}
80SaOl [15]	1203.357–1271.955	88/88/0	2.00×10^{-3}	1.64×10^{-3}
23EcSiFuRa (this work)	2290.876–2699.068	1603/1603/0	1.03×10^{-3}	7.83×10^{-4}
79WeSaLa [14]	3261.617–3871.973	402/401/0	1.50×10^{-3}	9.60×10^{-4}
94AzCaCrLo [20]	4168.031–10 438.322	1499/1499/0	5.22×10^{-3}	1.40×10^{-3}
93CaLoEsFu [19]	6770.942–7216.530	876/876/0	5.00×10^{-3}	8.90×10^{-4}
97ChDeHaAb [23]	11 413.643–11 510.052	352/352/0	5.00×10^{-3}	3.32×10^{-3}
96AbHaKaTr [22]	12 566.470–12 636.448	203/202/0	2.00×10^{-3}	1.24×10^{-3}
97HaChAbKo [24]	13 239.419–13 520.419	627/573/54	5.00×10^{-3}	2.81×10^{-3}

number of rovibrational states, a detailed checking is conducted to make sure that all the rovibrational labels are feasible and that they are internally consistent between the two HOCl isotopologues. Fourth, transitions based on empirical, EH, and variationally computed energy levels are supplemented with first-principles computed infrared intensities, allowing the straightforward assignment of new lines in the rovibrational spectrum of hypochlorous acid in the $2\nu_2$ region, where the experimental spectrum [11], measured in 1996, has remained available in electronic form. This procedure results in a number of newly assigned transitions and even new empirical energy levels, complementing nicely the work reported in Ref. [11]. The input sets of transitions for both isotopologues of HOCl are enlarged with the new transitions before the final MARVEL analysis. All the important results of the present study, including transitions and energy levels, are made available to the public in the extensive Supplementary Material (SM) to this paper.

2. Data sources

During this study, a concerted effort was made to collate *all* measured and assigned rovibrational transitions of $\text{H}^{16}\text{O}^{37}\text{Cl}$ available in the literature [11–26]. These experimental studies involve 13 bands. There is only one source known to us, 97ShNeZa [27], which contains transitions for $\text{H}^{16}\text{O}^{35}\text{Cl}$ but not for $\text{H}^{16}\text{O}^{37}\text{Cl}$; thus, the list of data sources treated is principally the same as that in Ref. [1]. The experimental sources used to construct the $\text{H}^{16}\text{O}^{37}\text{Cl}$ spectroscopic network of this study are given in Table 1.

Similar to $\text{H}^{16}\text{O}^{35}\text{Cl}$ [1], older literature sources may not contain the measured line positions of $\text{H}^{16}\text{O}^{37}\text{Cl}$ in an explicit form. As a result, these data could be considered lost to the community [28]. It is then important to note that (a) the line positions mentioned but not reported in Ref. [20] for $\text{H}^{16}\text{O}^{37}\text{Cl}$ are made available here to the public for the first time, (b) the original file containing the set of transitions measured and assigned for $\text{H}^{16}\text{O}^{37}\text{Cl}$ [11] got lost, and (c) transitions data for the $2\nu_2$ band of $\text{H}^{16}\text{O}^{37}\text{Cl}$ included in the Supplementary Material with the tag 23EcSiFuRa, referring to this paper, represent all the data of Ref. [11] plus a significant number of newly assigned transitions (*vide infra*).

This paper also reports a minor correction and extension of the data reported in Ref. [1] for $\text{H}^{16}\text{O}^{35}\text{Cl}$. In what follows, description of the data sources of the two HOCl isotopologues are given separately.

2.1. Notation

According to the usual convention [29], the ν_1 , ν_2 , and ν_3 vibrational fundamentals of HOCl correspond to the OH stretch, HOCl bend, and OCl stretch motions, respectively. HOCl, with an equilibrium structure

of C_s point-group symmetry, is only a very slightly asymmetric rotor, with a Ray-asymmetry parameter [30] of $\kappa = (2\bar{B} - \bar{A} - \bar{C})/(\bar{A} - \bar{C}) = -0.998$, where \bar{A} , \bar{B} , and \bar{C} are the rotational constants. Therefore, the measured spectra have the appearance of a prolate symmetric-top molecule with dominant *a*-type transitions. The rotational states of HOCl are labelled using the standard asymmetric-top quantum numbers J , K_a , and K_c [31]. As a result, the rovibrational labels of both HOCl isotopologues contain three vibrational and three rotational quantum numbers: $(\nu_1 \nu_2 \nu_3) [J K_a K_c] \equiv (\nu_1 \nu_2 \nu_3) J_{K_a K_c}$.

2.2. $\text{H}^{16}\text{O}^{35}\text{Cl}$

In 1969, 69LiLiMi [12] reported highly accurate measurements of the $1_{0,1} - 0_{0,0}$ rotational transition for several isotopologues of HOCl. This source was not included in the original MARVEL analysis of the $\text{H}^{16}\text{O}^{35}\text{Cl}$ isotopologue [1], but it is included in the present study.

The MARVEL analysis whose results are reported in Ref. [1] utilized 2108 lines from the Supplementary Material of the data source 00AuKlFlPa [26]. As it turned out, the transitions forming the ν_2 band, contained in the Supplementary Material of Ref. [26], are not the directly measured transitions but those based on EH energy values. An effort was made during this study to constrain the MARVEL analyses to measured data, which were published explicitly in Ref. [26] neither for $\text{H}^{16}\text{O}^{35}\text{Cl}$ nor for $\text{H}^{16}\text{O}^{37}\text{Cl}$. Prof. Vander Auwera, the first author of Ref. [26], kindly supplied these data to us. The data are now contained explicitly in the MARVEL input files of the two isotopologues. Dependable individual uncertainties were also provided by Vander Auwera for all the measured and assigned transitions of Ref. [26]. As a result, the number of transitions utilized in the MARVEL analysis of $\text{H}^{16}\text{O}^{35}\text{Cl}$ from the source 00AuKlFlPa [26] changed from 2108 to just 223; overall, the spectroscopic network (SN) shortened this way provides access to 564 less empirical rovibrational energy levels.

2.3. $\text{H}^{16}\text{O}^{37}\text{Cl}$

The number of rovibrational transitions collected from the literature, based on 15 sources, plus the results of the present study included in the MARVEL analysis of $\text{H}^{16}\text{O}^{37}\text{Cl}$ spectra is 10 266. We were able to validate 10 124 of these transitions *via* a detailed MARVEL-based analysis. Note that if a transition is not part of the principal component of the SN, we are not able to validate it. Table 1, displaying the full list of data sources used during the MARVEL analysis of this study, along with some data characteristics, also contains the information how many transitions we had to delete from each source (see the available (*A*)/validated (*V*)/deleted (*D*) column). Table 1 also contains *AMR* (average MARVEL reproduction) values, showing how well, in an

Table 2

Harmonic vibrational fundamentals (ω_i , given in brackets) and selected anharmonic vibrations (ν_i , including fundamentals, overtones, and combination bands) of $\text{H}^{16}\text{O}^{35}\text{Cl}$ and $\text{H}^{16}\text{O}^{37}\text{Cl}$, all in cm^{-1} , obtained at two levels of electronic-structure theory: MP2 = frozen-core aug-cc-pVTZ MP2 and CC = frozen-core aug-cc-pV(Q+d)Z CCSD(T). There is no direct experimental information available for the fundamentals of $\text{H}^{16}\text{O}^{37}\text{Cl}$, the only experimentally known combination or overtone vibrational band origin is $\nu_1 + \nu_3$ at $4325.74(1) \text{ cm}^{-1}$, as revealed during this study. For the experimental results, the uncertainties are given in parentheses.

$\nu_i(\omega_i)$	$\text{H}^{16}\text{O}^{35}\text{Cl}$		Experiment [1]	$\text{H}^{16}\text{O}^{37}\text{Cl}$	
	MP2	CC		MP2	CC
$\nu_1[\omega_1]$	3593.6[3771.2]	3610.2[3796.1]	3609.479 7(30)	3593.7[3771.2]	3610.2[3796.1]
$\nu_2[\omega_2]$	1227.7[1260.6]	1238.3[1271.8]	1238.624 7(4)	1227.2[1260.1]	1237.8[1271.3]
$\nu_3[\omega_3]$	752.2[765.4]	726.3[741.4]	724.358 2(6)	745.8[758.8]	720.1[735.0]
$2\nu_3$	1496.9	1442.8		1484.1	1430.6
$\nu_2 + \nu_3$	1971.7	1955.5		1964.9	1949.0
$2\nu_2$	2440.1	2460.7		2439.0	2459.7
$\nu_1 + \nu_3$	4342.9	4334.5	4331.9090(8)	4336.5	4328.3
$\nu_1 + \nu_2$	4794.7	4822.5		4794.1	4822.0
$2\nu_1$	7024.5	7048.5		7024.5	7048.5

average sense, the MARVEL energy levels are able to reproduce the experimentally measured lines of the given source. It is not surprising that for most sources the empirical (MARVEL) energy levels can reproduce the measured lines within the experimental uncertainties, indicating that the cleansed MARVEL database of $\text{H}^{16}\text{O}^{37}\text{Cl}$ contains only a limited number of even slightly conflicting transitions. Since MARVEL performs a weighted fit, preferring the best measurements, it is also not surprising to see AMR values almost always significantly smaller than the AIU (average initial uncertainty) values.

There is only one data source, 97HaChAbKo [24], where measured transitions had to be deleted. Similar to the analysis of the spectra of the $\text{H}^{16}\text{O}^{35}\text{Cl}$ isotopologue [1], we had to remove the complete set of experimental information available on the $4\nu_1 + \nu_2$ band in this source, since these 54 transitions exhibit unresolvable conflicts among themselves.

As seen in Table 1, apart from 80 transitions of 00AuKIFIPa [26], almost all of the measured and assigned transitions found in the literature could be validated during this study. The further exceptions are as follows: one transition in each of 79WeSaLa [14], 86LaOl [17], and 96AbHaKaTr [22], and five transitions of 98FlBiWaOr [25]. All these transitions, which could not be validated as they are not part of the principal component of the spectroscopic network, may be connected to the principal component with a limited number of well-designed experiments [32] in the future.

2.4. Experimental spectrum of the $2\nu_2$ band of HOCl

The measured spectrum of HOCl in the $2\nu_2$ region, that is between 2290 and 2700 cm^{-1} , was not published originally in Ref. [11]. Nevertheless, the spectrum measured in 1996 [11] was kept by the authors in electronic form, allowing its reanalysis. The experimental conditions under which the spectrum was measured are given in Ref. [11]. During this study, the $2\nu_2$ band is reanalyzed, based on empirical (MARVEL) and effective Hamiltonian (EH) rovibrational energies and first-principles computed transitions and intensities (*vide infra*).

3. The simple HO and VPT2 picture

Computational quantum-chemical studies performed on HOCl [33–50], including variational ones [39,46,47,49], have yielded a detailed basic understanding of the energy-level structure and the associated rovibrational spectra of $\text{H}^{16}\text{O}^{35}\text{Cl}$, and to some extent of $\text{H}^{16}\text{O}^{37}\text{Cl}$. Nevertheless, as part of the present study, the simplest theoretical models, namely the harmonic-oscillator (HO) approximation [51] and vibrational perturbation theory carried out to second order (VPT2) [52–54], have been used to obtain harmonic and anharmonic vibrational results for the two isotopologues.

The simple HO and VPT2 results obtained, presented in Table 2, show that for HOCl (a) the spectroscopic data obtained at the frozen-core aug-cc-pV(Q+d)Z CCSD(T) level [55,56] show excellent agreement

Table 3

Information related to the type and the number of discrete-variable-representation vibrational basis functions and the range of the coordinate grid employed for each internal coordinate during the quantum-chemical computations.

	r_{OCl}	r_{OH}	θ
Basis type	Hermite	Hermite	Legendre
Number of basis functions	70	20	50
Coordinate interval	1.4 Å–2.8 Å	0.6 Å–1.9 Å	46° – 179°

with the available experimental data, with deviations less than 2 cm^{-1} obtained within the VPT2 formalism for the three fundamentals of $\text{H}^{16}\text{O}^{35}\text{Cl}$, and similar agreement is expected for $\text{H}^{16}\text{O}^{37}\text{Cl}$, for which no truly experimental results are available, (b) isotopic substitution has a negligible effect on the ν_1 fundamental (0.0 cm^{-1}), a minimal effect on ν_2 (0.5 cm^{-1}), and a somewhat significant effect on ν_3 (6.2 cm^{-1}), which is the O–Cl stretch fundamental, (c) as proven for the $\nu_1 + \nu_3$ combination band, the discrepancy at the aug-cc-pV(Q+d)Z CCSD(T) level compared to experiment is the same for the two isotopologues, and (d) the isotope shifts appear to be almost perfectly additive for the overtone and combination modes. The minuscule ν_1 isotopic shift is due to the decoupling of the OH stretch motion from the other two vibrational motions and to the fact that the a axis is more or less aligned with the O–Cl bond. These elementary results help to understand the assignment of the rovibrational quantum states of hypochlorous acid, discussed at considerable length in later parts of this paper.

4. Variational nuclear-motion computations

In order to check the energy levels and the rovibrational labels available in the literature for $\text{H}^{16}\text{O}^{35}\text{Cl}$ and $\text{H}^{16}\text{O}^{37}\text{Cl}$, independent first-principles nuclear-motion computations have been performed for the two molecules. These computations utilized our version of the fourth-age [57] quasivariational quantum-chemical code GENIUSH [58–60], where the abbreviation stands for GEneral rovibrational code with Numerical, Internal-coordinate, User-Specified Hamiltonians.

The internal coordinates chosen to describe the nuclear dynamics of HOCl are as follows (see Table 3): O–Cl stretch (r_{OCl}), O–H stretch (r_{OH}), and HOCl bend (θ). The rovibrational wavefunctions are expanded in the direct product of vibrational and rotational basis functions. A complete set of $2J + 1$ orthonormal Wang functions [30] form the rotational basis. Table 3 contains information about the type and the number of discrete variable representation (DVR) [61,62] vibrational basis functions, and the range of the coordinate grid, employed during this study. The empirically-adjusted potential energy surface (PES) developed in Ref. [33] and the dipole-moment surface (DMS) of Ref. [63] were used in this study. The nuclear masses, in u, employed during the variational computation of the rovibrational states are as follows: $m(\text{H}) = 1.007 825$, $m(^{16}\text{O}) = 15.994 915$, $m(^{35}\text{Cl}) = 34.968 852 69$, and $m(^{37}\text{Cl}) = 36.965 902 6$.

Table 4

The first 50 vibrational eigenenergies computed for the two HOCl isotopologues, in cm^{-1} , based on the empirically-adjusted potential energy surface of Ref. [33] and an exact kinetic-energy operator (the (000) values are the zero-point vibrational energies (ZPVE), all other energies are reported relative to the ZPVEs).

ν_1	ν_2	ν_3	$\text{H}^{16}\text{O}^{35}\text{Cl}$	$\text{H}^{16}\text{O}^{37}\text{Cl}$
0	0	0	2867.0	2863.5
0	0	1	724.3	718.1
0	1	0	1238.6	1238.1
0	0	2	1444.1	1431.8
0	1	1	1953.8	1947.2
0	0	3	2154.0	2135.8
0	2	0	2456.4	2455.3
0	1	2	2663.3	2650.7
0	0	4	2852.2	2828.3
0	2	1	3163.8	3156.8
0	1	3	3362.3	3344.0
0	0	5	3537.1	3507.8
1	0	0	3610.0	3610.0
0	3	0	3670.4	3668.8
0	2	2	3865.9	3853.0
0	1	4	4049.2	4025.4
0	0	6	4208.8	4174.4
1	0	1	4334.0	4327.8
0	3	1	4368.7	4361.2
0	2	3	4556.7	4538.2
0	1	5	4723.3	4694.2
1	1	0	4822.0	4821.5
0	0	7	4868.2	4828.8
0	4	0	4878.9	4876.8
1	0	2	5053.3	5040.9
0	3	2	5062.0	5048.8
0	2	4	5235.0	5211.0
0	1	6	5384.8	5350.6
0	0	8	5515.9	5471.7
1	1	1	5535.8	5529.1
0	4	1	5566.3	5558.5
0	3	3	5743.0	5724.2
1	0	3	5763.3	5745.0
0	2	5	5900.1	5870.9
1	2	0	6014.8	6013.8
0	1	7	6034.8	5995.6
0	5	0	6073.9	6071.2
0	0	9	6152.4	6103.6
1	1	2	6242.0	6229.0
0	4	2	6250.9	6237.9
0	3	4	6411.0	6386.9
1	0	4	6460.6	6436.8
0	2	6	6552.6	6518.4
0	1	8	6673.6	6629.6
1	2	1	6718.3	6711.2
0	5	1	6748.8	6740.5
0	0	10	6778.0	6724.8
0	4	3	6916.5	6897.6
1	1	3	6945.0	6926.7
2	0	0	7050.4	7050.4
0	3	5	7065.2	7035.9

Table 4 lists the first 50 vibrational eigenenergies computed for the two HOCl isotopologues. When a comparison can be made, these vibrational energies are the same as reported in Refs. [33] and [39]. The order of the state energies in Table 4 follows that of $\text{H}^{16}\text{O}^{35}\text{Cl}$. The density of vibrational states is relatively low even at 7000 cm^{-1} . Nevertheless, in a couple of cases, in fact for the vibrational state pairs (1 2 0)/(0 1 7), (0 5 1)/(0 0 10), and (2 0 0)/(0 3 5), the order changes between $\text{H}^{16}\text{O}^{35}\text{Cl}$ and $\text{H}^{16}\text{O}^{37}\text{Cl}$, suggesting significant mixing in states where the O–Cl stretch (ν_3) is highly excited.

Although the accuracy of the computed absolute rovibrational eigenenergies is insufficient to employ them directly to check the accuracy of the empirical energy levels, they can be utilized to obtain energy differences between rovibrational states of the two isotopologues with the same label. The accuracy of the differences improves to the expected full width at half maximum of the infrared lines observed at room

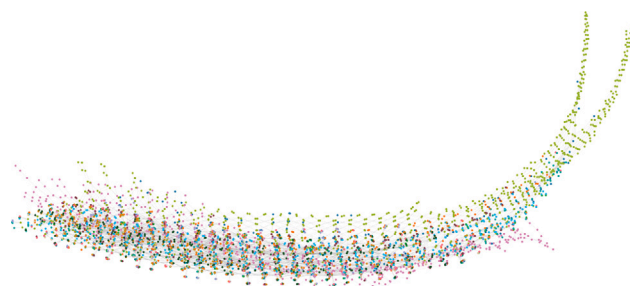


Fig. 1. Cartoon about the spectroscopic network (SN) of $\text{H}^{16}\text{O}^{37}\text{Cl}$, with each band represented by a different colour. The SN of $\text{H}^{16}\text{O}^{35}\text{Cl}$ is highly similar.

temperature, a few times 10^{-2} cm^{-1} . This improved relative accuracy with respect to the absolute accuracy is due to the following factors: (a) errors coming from the imperfect treatment of the vibrations, like inaccuracy of the PES, more or less cancel each other out when the difference is taken between the energy levels with the same vibrational label, and (b) there is no error in the treatment of the rotation due to the use of a complete rotational basis.

The computed rovibrational wave functions were utilized within the rigid-rotor decomposition (RRD) approach [64,65] to determine rotational labels for all the rovibrational states. The RRD calculations were done in the Eckart embedding [66–68]. In the Eckart embedding unique labels could be attached unambiguously to the states computed. The GENIUSH computations have been carried out up to $J_{\text{max}} = 45$ and the list of states is complete up to 3000 cm^{-1} . Determination of the one-photon, dipole-allowed intensities for both HOCl isotopologues was based on the computed rovibrational eigenvectors.

5. MARVEL analysis of the measured transitions

The MARVEL protocol [4,5,7] inverts the information contained in uniquely assigned experimental transitions and yields what are called empirical rovibrational energies, all with well-defined provenance and uncertainty. There are ample studies even for systems larger than triatomic ones [69–72] demonstrating the utility of the MARVEL approach for the spectroscopic community and beyond. There is a review available about the technique [10], and one should also note that results from several MARVEL analyses have been included in the latest editions of HITRAN [2,3].

The experimental uncertainties of the measured transitions, which are part of the input to MARVEL, allow an estimation of the uncertainties of the empirical rovibrational energy levels. These data, that is experimental transitions with assignments and uncertainties and empirical rovibrational energy levels with assignments and uncertainties, are contained in the SM to this paper.

Due to the fact that HOCl contains three different nuclei, the experimental spectroscopic networks of HOCl isotopologues, built from the assigned transitions, have a single principal component. The principal component of $\text{H}^{16}\text{O}^{37}\text{Cl}$ contains more than 10 000 transitions, formed by almost 4000 energy levels. There are 49 much smaller, floating components, containing altogether 49 states and 88 transitions. Fig. 1 provides a representation of the spectroscopic network of $\text{H}^{16}\text{O}^{37}\text{Cl}$. As usual in graph (network) theory, the actual shape of the figure has no specific meaning; in particular, there is no energy axis associated with this figure. Each vibrational band is represented with a different colour. The large number of energy levels with a single measured transition ('leaves') and the large number of even-membered cycles, allowing the straightforward assessment of various experimental results, are clearly visible.

Table 5
MARVEL-based vibrational band origins (VBO) of H¹⁶O³⁷Cl and effective Hamiltonian results from the literature.^a

Band	VBO			N_{RL}	J_{max}	$K_{a,\text{max}}$
	MARVEL	Previous estimates ^b	Ref.			
v_0	0.0(0)	0.0	–	866	56	10
v_3	–	718.165 819(15)	[25]	445	37	7
v_2	–	1238.121 286(10)	[25]	181	39	5
$2v_2$	–	2460.190 020(75) ^c	[11]	371	39	5
v_1	–	3609.488 960(30)	[25]	239	48	8
$v_1 + v_3$	4325.74(1)	4325.742 131(210)	[20]	256	30	5
$v_1 + v_2$	–	4819.932 145(257)	[20]	210	30	5
$v_1 + 2v_2$	–	6012.762 757(783)	[20]	172	32	3
$2v_1$	–	7049.823 393 7(935)	[19]	295	34	5
$3v_1$	10 322.374(6)	10 322.377 81(113)	[20]	198	36	6
$3v_1 + v_2$	11 477.433(5)	11 477.452(1)	[23]	253	40	4
$3v_1 + 2v_2$	–	12 611.475 7(12)	[22]	164	36	4
$4v_1$	–	13 427.364 1(6)	[24]	305	38	5

^a All VBO values are given in cm⁻¹. The uncertainties of the last VBO digits are given in parentheses. The number of rotational levels, N_{RL} , and the maximum J and K_a values within a given vibrational band (Band) are given in the last three columns of this table.

^b The previous (best) estimates are based on effective Hamiltonian calculations. For higher-excited states the uncertainty of the VBOs may not reflect correctly their accuracy.

^c In this work, a new effective Hamiltonian value, consistent within the uncertainties given, has been determined for this VBO: 2460.190 186 6(765) cm⁻¹ (see Table 6).

6. Results and discussion

6.1. Vibrational band origins of H¹⁶O³⁷Cl

Vibrational band origins (VBO) and empirical rovibrational energies, complementing those of H¹⁶O³⁷Cl discussed here, are available for H¹⁶O³⁵Cl from Ref. [1]. These VBOs are not discussed explicitly in what follows. Table 5 presents the VBOs and a summary of the number of empirical rovibrational energy levels determined for each vibrational parent state of H¹⁶O³⁷Cl. Interestingly, none of the vibrational fundamentals of H¹⁶O³⁷Cl are known experimentally, as the $J = 0$ states have not been involved in measured transitions, but relatively accurate energies are determined for one overtone and two combination bands.

Table 5 also gives term values for 13 vibrational states, including the ground state, of H¹⁶O³⁷Cl. These results are based on EH calculations [11,19,20,22–25]. There are only three cases, $v_1 + v_3$, $3v_1$, and $3v_1 + v_2$, where the empirical and the EH estimates can be compared. The values agree within the MARVEL uncertainties for two cases but not for $3v_1 + v_2$. The related transition was measured by 97HaChAbKo [23], whose EH fit reproduced the $3v_1 + v_2$ VBO only within 0.019 cm⁻¹. Overall, the stated uncertainties of the EH estimates are significantly less than those coming from the MARVEL analysis. Since the EH analyses are based on a large number of measured rovibrational transitions, see the column N_{RL} of Table 5, the EH uncertainties may in fact be better than just simple statistical measures of the goodness of the EH fit.

6.2. Empirical rovibrational energies of H¹⁶O³⁵Cl and H¹⁶O³⁷Cl

Based on the measured and assigned rovibrational transitions published in 16 sources (see Table 1), we obtained empirical energies for 3933 rovibrational states of H¹⁶O³⁷Cl (this is the sum of the N_{RL} values, that is the number of rotational levels, of Table 5). The full list is provided, along with the quantum numbers assigned to the states, in the SM to this paper. The largest rotational quantum number is $J_{\text{max}} = 56$, corresponding to the vibrational ground state, while the rovibrational energies extend up to 14 566 cm⁻¹ (on the (4 0 0) vibrational parent state). It is interesting that, due to the large value of the rotational constant A , the maximum value of K_a is only 10, i.e., there are no measured transitions in the literature which involve a state with a K_a value larger than 10 (see the last column of Table 5 how limited the K_a coverage is, the largest value is on the vibrational ground state). Apart from the fact that all energy levels with $K_a > 10$ are missing in the experimental transitions list, (000)13_{10,3} is the first missing state.

The uncertainties of the empirical rovibrational energy levels derived clearly show the lack of a significant number of connected MW measurements on HOCl. For example, there is only one energy level whose uncertainty is less than 3×10^{-5} cm⁻¹, that is 1 MHz. The uncertainties of all the other empirical rovibrational energy levels are larger than 2×10^{-4} cm⁻¹.

Fig. 2 shows the differences between the empirical energy levels of this study and the EH results of 98FIBiWaOr [25] for four bands (v_0 , v_1 , v_2 , and v_3), for H¹⁶O³⁵Cl (top panel) and H¹⁶O³⁷Cl (bottom panel). Almost all of the differences are in the expected range. The only feature worth discussing concerns the (0 1 0) $\equiv v_2$ rovibrational levels of H¹⁶O³⁵Cl. Clearly, there are several levels, all between 1800–2000 cm⁻¹, which have unacceptably large discrepancies. There are no similar discrepancies for H¹⁶O³⁷Cl. It is important to point out that even in the original source, 86LaOl [17], whose data were treated in 98FIBiWaOr [25], these energy levels could not be reproduced within 0.005 cm⁻¹. The problem is caused by a Coriolis-type resonance between the (0 1 0) and the (0 0 2) vibrational states at $K_a = 5$ around $J = 20$, and this is discussed in detail in Ref. [25].

6.3. Comparison of the empirical rovibrational energy levels of H¹⁶O³⁵Cl and H¹⁶O³⁷Cl

Since the density of vibrational states of HOCl is low in the infrared region, providing the ($v_1 v_2 v_3$) labels as the vibrational parents of rovibrational states is straightforward. Furthermore, using the RRD procedure [64,65] in the Eckart embedding [67] results in straightforward rotational labels. The “only” difficulty when trying to match empirical and first-principles labels of rovibrational states is the relatively large discrepancy of the computed results. Nevertheless, this matching was done successfully for both isotopologues.

The next step is to consolidate the empirical energies derived for H¹⁶O³⁵Cl and H¹⁶O³⁷Cl through our MARVEL-based studies, augmented with EH and variational results. There are close to 4000 energy levels that are available for both isotopologues and which we could compare. This procedure involved several steps and several different datasets. The main points are discussed below.

Fig. 3 provides a rough comparison between the empirical rovibrational energy levels of H¹⁶O³⁵Cl and H¹⁶O³⁷Cl by plotting differences between the energies of the same states of the two isotopologues (governed by their assignment) as a function of the rotational quantum number J . Only the four most important vibrational parent states are covered in Fig. 3: (0 0 0), (0 0 1), (0 1 0), and (1 0 0). This figure is not very insightful when fine details are considered but shows that there

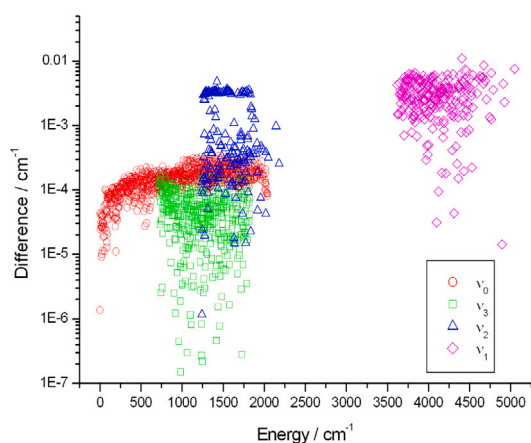
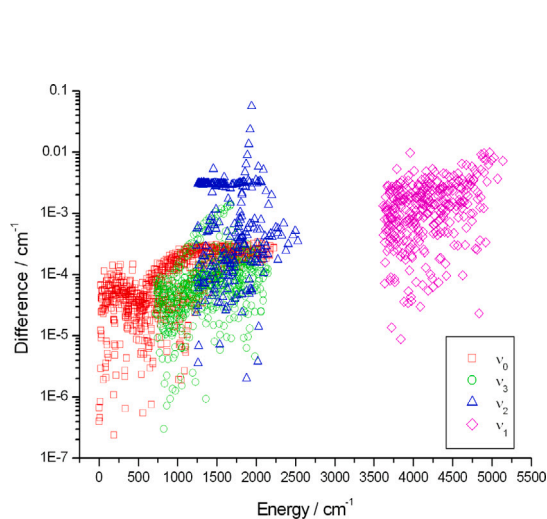


Fig. 2. Differences between the empirical (MARVEL) energy levels of this study and the earlier literature results of 98FIBiWaOr [25] on the vibrational ground state (ν_0) and the vibrational fundamentals (ν_1 , ν_2 , and ν_3) of $\text{H}^{16}\text{O}^{35}\text{Cl}$ (top panel) and $\text{H}^{16}\text{O}^{37}\text{Cl}$ (bottom panel).

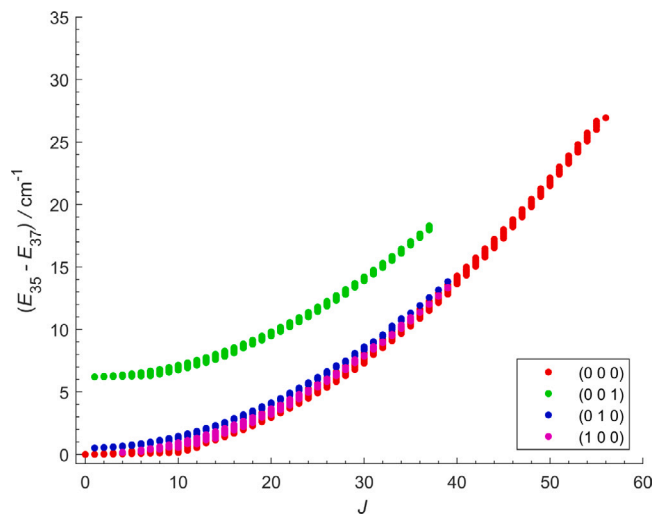
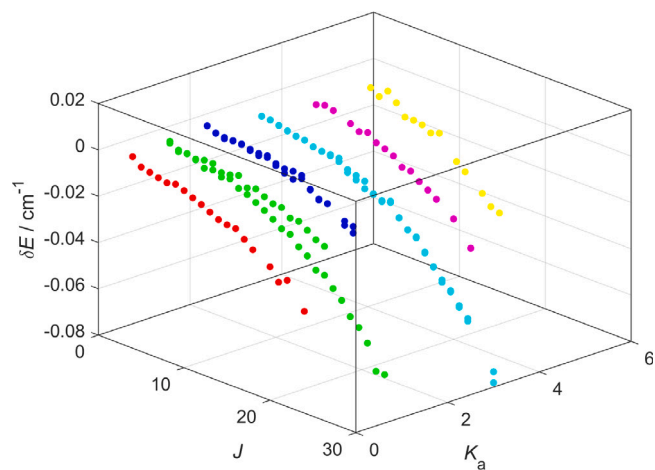
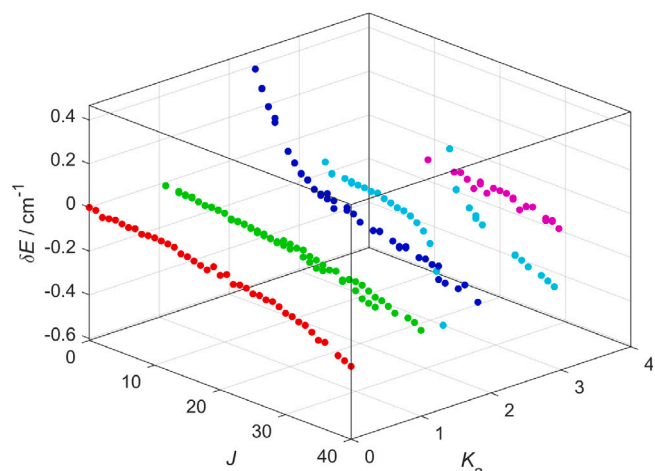


Fig. 3. Differences between the $\text{H}^{16}\text{O}^{35}\text{Cl}$ and $\text{H}^{16}\text{O}^{37}\text{Cl}$ empirical rovibrational energy levels as a function of the J rotational quantum number for a few vibrational bands (see the insert).



(a) $\nu_1 + \nu_2 \equiv (1\ 1\ 0)$ state



(b) $3\nu_1 + \nu_2 \equiv (3\ 1\ 0)$ state

Fig. 4. Differences between the MARVEL and the rigid-rotor isotopologue shifts (δE), as a function of J and K_a , for the (1 1 0) and (3 1 0) vibrational states. For the panels a and b, the K_a values range from 0 to 5 and to 4, respectively. The different K_a points are represented with different colours.

are no major issues with the assignments and that the rovibrational energy differences show strong (nearly quadratic) J dependence. Clearly, better ways to display the data are needed if one were to find possible discrepancies between the empirical rovibrational energies of $\text{H}^{16}\text{O}^{35}\text{Cl}$ and $\text{H}^{16}\text{O}^{37}\text{Cl}$.

To detect possible minor issues with the data, we compared the rigid rotor and the empirical (MARVEL) isotopologue shifts by plotting their differences, δE , against the J and the K_a rotational quantum numbers. The rigid-rotor isotopologue shift was calculated using the ground-state rotational constants reported in Ref. [73]. The plots generated for the different vibrational states covered in our study confirm that the rigid-rotor model is adequate for the semirigid HOCl isotopologues and helps to observe possible misassignments.

As an example, Fig. 4(a) contains data regarding the (1 1 0) vibrational state. It is important to point out that in Fig. 4(a) the experimental uncertainties show up as rugged δE “lines” for a given K_a . As to the consistency of the $\text{H}^{16}\text{O}^{35}\text{Cl}$ and $\text{H}^{16}\text{O}^{37}\text{Cl}$ energy levels, an outlier data point would suggest that there is a problem with the energy level of one of the isotopologues. Fig. 4(b) contains data regarding the (3 1 0) vibrational state. In Fig. 4(b), systematic deviations can be observed at $K_a = 3$ and $K_a = 4$, indicating some sort of resonances in the energy levels of the $\text{H}^{16}\text{O}^{35}\text{Cl}$ isotopologue. These transitions were measured

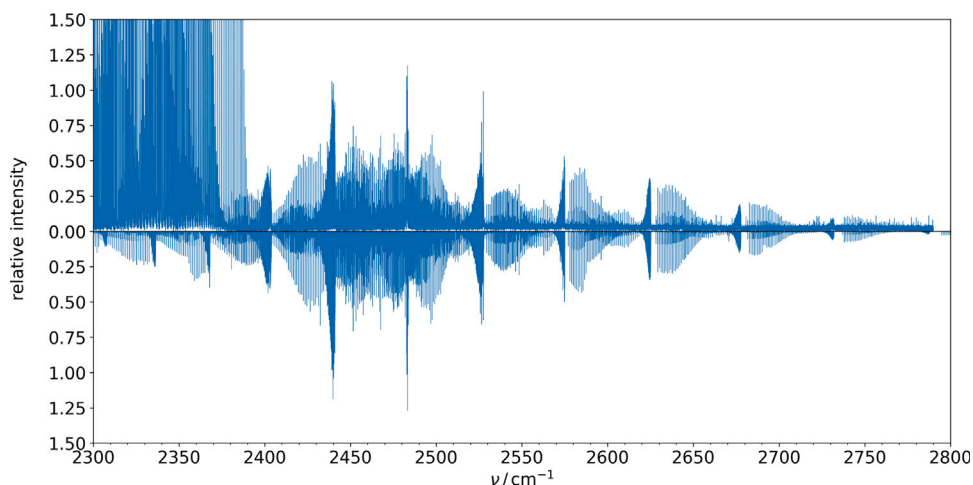


Fig. 5. Overview of the room-temperature, baseline-corrected measured (upper panel) and calculated (lower panel) spectrum of HOCl in the 2300–2800 cm^{-1} region. The intensities are arbitrarily normalized by the intensity of an intensive transition at 2480 cm^{-1} . Below about 2400 cm^{-1} the high-intensity observed lines are due to CO_2 .

by 97ChDeHaAb [23], who detected and analysed these deviations and found that these energy levels are perturbed by the (2 2 3) state. The two panels of Fig. 4, and similar plots for other bands (taking into account perturbations like the one discussed), confirm that at the end of our validation procedure no obvious outliers remain in the MARVEL datasets of the two HOCl isotopologues.

7. New assignments in the $2\nu_2$ band region

At this point, we have validated transitions and empirical energy levels for both HOCl isotopologues. Since accurate first-principles and EH modelling results are also available, checking and extending the assignment of the dipole-allowed spectrum of the two isotopologues in the $2\nu_2$ band region, first presented and discussed in Ref. [11], can now be performed. The procedure followed starts with the complete set of first-principles-computed lines (generation of the lines from the rovibrational states computed is governed by the usual one-photon, dipole-allowed selection rules). In the next step, the energies involved in these transitions are replaced by their MARVEL and, when not available, the EH equivalents, both for the (0 0 0) and the (0 2 0) vibrational states. This procedure ensures completeness and accuracy at the same time. Comparison of the measured spectrum with the one calculated the way described is given in Fig. 5. The calculated spectrum (the lower panel of Fig. 5) was generated from the calculated line list assuming a Gaussian lineshape with a half width at half maximum of 0.003 cm^{-1} . The high quality of the calculated spectrum is perfectly clear, especially notable is the impressive agreement between the measured and computed intensities (this scale does not allow to detect irregularities in the prediction of the line centre positions). Under about 2400 cm^{-1} the experimental spectrum is contaminated with transitions belonging to the CO_2 molecule. Note that in certain parts of the spectrum, as usual, H_2O lines can also be found.

The panels of Fig. 6 illustrate old and new assignments in the 2615 – 2670 cm^{-1} section of the $2\nu_2$ band of HOCl. Old assignments, given in Ref. [11], are indicated with grey dashed vertical lines. The red and blue dashed vertical lines of Fig. 6 correspond to new assignments made for $\text{H}^{16}\text{O}^{35}\text{Cl}$ and $\text{H}^{16}\text{O}^{37}\text{Cl}$, respectively.

In Fig. 6, solid vertical lines represent the calculated transitions, with first-principles normalized intensities and MARVEL and EH wavenumbers, as explained earlier. These lines are blue if the transition belongs to $\text{H}^{16}\text{O}^{37}\text{Cl}$. Green and red lines belong to $\text{H}^{16}\text{O}^{35}\text{Cl}$; green, if both the upper and lower energy levels were already present in the MARVEL database reported in Ref. [1], and red in all the other cases (only one, or none of the two energy levels were present).

In Fig. 6(a), the Q and R subbranches of the $K'_a = 4 \leftarrow K''_a = 3$ branch can be seen. Fig. 6(b) shows more details about the Q subbranch. $\text{H}^{16}\text{O}^{37}\text{Cl}$ transitions superimposed on the $\text{H}^{16}\text{O}^{35}\text{Cl}$ transitions can be observed. The tail of the Q subbranch is plotted in Fig. 6(c). It can be seen that beside the $\text{H}^{16}\text{O}^{37}\text{Cl}$ transitions (plotted with blue), there are numerous newly assigned $\text{H}^{16}\text{O}^{35}\text{Cl}$ transitions in this region (plotted with red dashed lines). Looking at the $\text{H}^{16}\text{O}^{35}\text{Cl}$ transition at around 2621.2 cm^{-1} , it can be seen that the corresponding two energy levels were already available in the MARVEL database (the calculated line plotted is green). Consequently, no new energy levels could be added to the MARVEL database by assigning this transition. In Fig. 6(c), on the other hand, there are newly assigned $\text{H}^{16}\text{O}^{35}\text{Cl}$ transitions for which the calculated (solid) lines are in red. This means that these transitions define new energy levels previously unknown empirically. The newly assigned experimental transitions are part of the MARVEL input and output files with the tag ‘23EcSiFuRa’, referring to this paper.

As a final step of our study, effective Hamiltonian parameters, corresponding to the $2\nu_2$ state, have been fitted to all the experimental data of the two HOCl isotopologues. The ground state (GS) term values used to calculate the transition wavenumbers were obtained from the parameters listed in Table 1 of Ref. [11]. The usual Watson-type Hamiltonian [74], in the S reduction and I' representation, containing terms up to the eighth power in the angular momentum, was adopted for the analysis. In the least-squares analyses, unit weights were assigned to experimental data corresponding to isolated lines. In the case of overlapping lines, half weights were assigned to the two transitions, using the average of the corresponding calculated wavenumbers as calculated value. Several fits were performed refining different sets of parameters. In each cycle of the fitting procedure, the transition wavenumbers differing from their calculated counterparts by more than a chosen rejection limit, which was gradually decreased from one iteration to the next, were excluded from the data set. After each iteration, the statistical significance as well as the correlation coefficients of the parameters obtained was checked. With a chosen limit of rejection of 0.002 cm^{-1} (five times the estimated experimental uncertainty), 166 of 2661 data values for $\text{H}^{16}\text{O}^{35}\text{Cl}$ and 40 of 1491 for $\text{H}^{16}\text{O}^{37}\text{Cl}$, corresponding to 6.2% and 2.7%, respectively, were excluded in the last cycle. The discarded transitions are randomly distributed and they are poorly measured or blended lines.

The refined spectroscopic parameters of the optimal fit are collected in Table 6, together with the GS parameters, listed for completeness. The parameters are statistically well determined and are at least three times larger than their uncertainties. All parameters of the model were allowed to vary during the fitting and were constrained to zero if they turned out to be statistically undetermined or did not improve

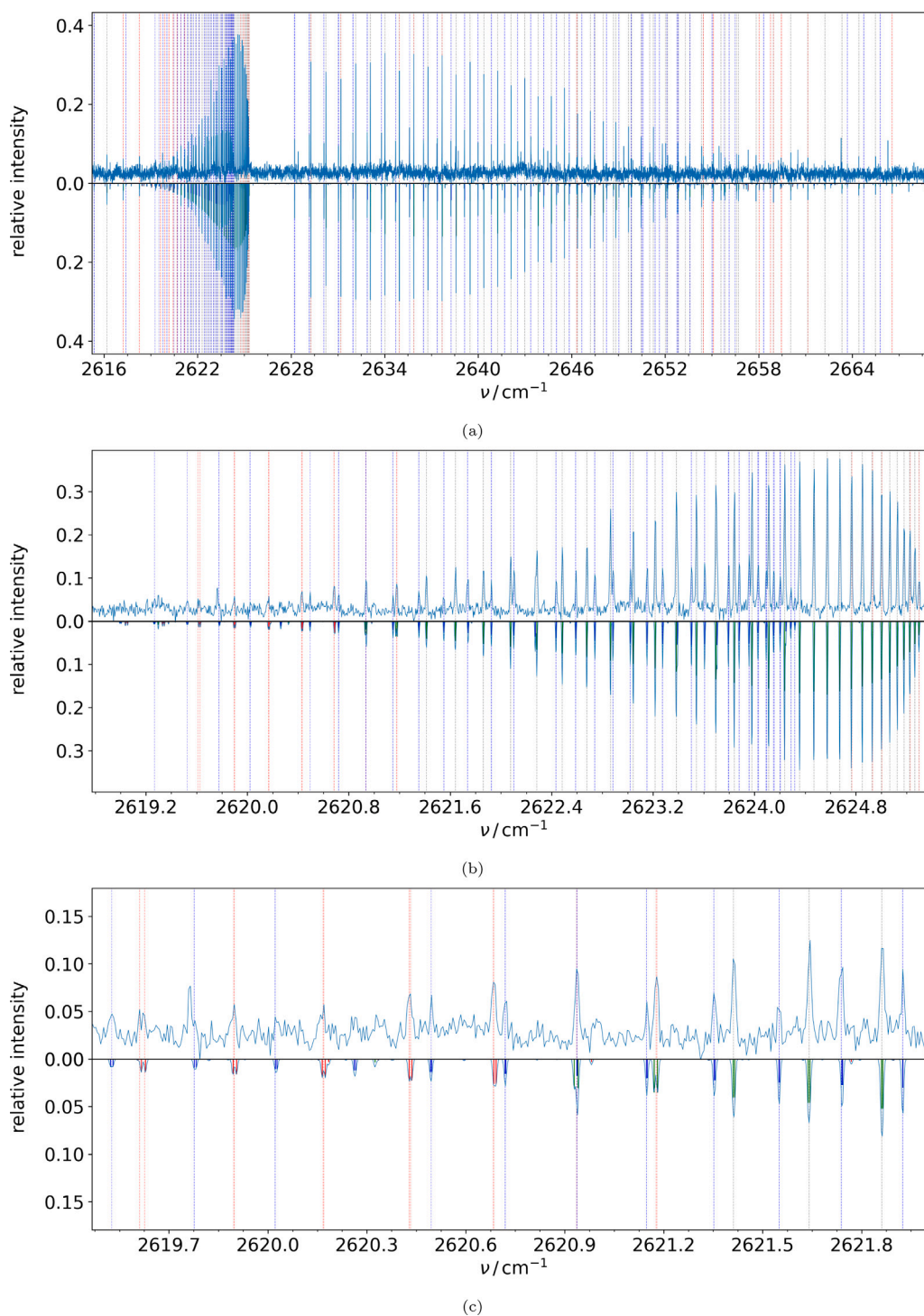


Fig. 6. Three sections of the $K'_v = 4 \leftarrow K'' = 3$ branch of the spectrum of HOCl, with different dispersion and with baseline adjustment. On all panels the measured and the calculated spectra are plotted on the upper and the lower subpanels, respectively. The blue solid vertical lines represent the calculated $\text{H}^{16}\text{O}^{37}\text{Cl}$ lines. The green and red solid vertical lines denote $\text{H}^{16}\text{O}^{35}\text{Cl}$ transitions. The line is green if the corresponding energy levels are present in the earlier MARVEL database [1], and red otherwise. The dashed lines denote the assigned transitions. In the case of the $\text{H}^{16}\text{O}^{37}\text{Cl}$ transitions the vertical lines are blue. The grey and red dashed lines represent $\text{H}^{16}\text{O}^{35}\text{Cl}$ transitions reported previously and assigned in this work, respectively.

the quality of the reproduction of the data. The standard deviations of an observation of unit weight reported in the table, 0.00059 cm^{-1} for $\text{H}^{16}\text{O}^{35}\text{Cl}$ and 0.00069 cm^{-1} for $\text{H}^{16}\text{O}^{37}\text{Cl}$, compare well with the estimated uncertainty of the experimental data, 0.0004 cm^{-1} . Significant correlations have been observed between a few high/low-order parameters. For $\text{H}^{16}\text{O}^{35}\text{Cl}$, the H_J/D_J , H_K/D_K , and L_{KKJ}/H_{KJ} pairs

are 97% correlated, L_K/H_K is 98% correlated, while for $\text{H}^{16}\text{O}^{37}\text{Cl}$, H_J/D_J and H_K/D_K are 96% correlated.

The internal consistency of the corresponding $\text{H}^{16}\text{O}^{35}\text{Cl}$ and $\text{H}^{16}\text{O}^{37}\text{Cl}$ parameters has also been evaluated. The percentage differences of the B , D , and d values, except d_2 , amount to less than 2, 4, and 10%, respectively. Much larger differences are observed for the H

Table 6

Spectroscopic parameters, in cm^{-1} , for the $2\nu_2$ and the ground (GS) vibrational states of $\text{H}^{16}\text{O}^{35}\text{Cl}$ and $\text{H}^{16}\text{O}^{37}\text{Cl}$ in the I' representation and S reduction. NFAD = number of fitted/assigned data, SDO = standard deviation of observations of unit weight.^a

Parameter	$2\nu_2(\text{H}^{16}\text{O}^{35}\text{Cl})$	$2\nu_2(\text{H}^{16}\text{O}^{37}\text{Cl})$	GS($\text{H}^{16}\text{O}^{35}\text{Cl}$)	GS($\text{H}^{16}\text{O}^{37}\text{Cl}$)
E	2461.2223868(527)	2460.1901866(765)	–	–
B_x	0.502724596(310)	0.493836372(589)	0.50424182889	0.49535739206
B_y	0.487066366(305)	0.478710860(603)	0.49119909287	0.48276399270
B_z	22.0883275(235)	22.0870829(279)	20.4636159483	20.4628665568
$D_J \times 10^6$	0.922187(291)	0.885388(743)	0.89730446	0.86661280
$D_{JK} \times 10^4$	0.532001(299)	0.512738(476)	0.41767208	0.40605707
$D_K \times 10^2$	0.814155(303)	0.806492(261)	0.433953889	0.433877729
$d_1 \times 10^7$	–0.255800(686)	–0.24069(215)	–0.20894225	–0.19832750
$d_2 \times 10^8$	–0.30843(301)	–0.27734(789)	–0.1504877	–0.1385825
$H_J \times 10^{12}$	–0.3117(975)	–2.986(369)	–0.573824	–0.59915
$H_{JK} \times 10^9$	0.1546(123)	–1.600(244)	0.1011978	0.0985742
$H_{KJ} \times 10^6$	0.10346(196)	0.06458(168)	0.02682989	0.0253971
$H_K \times 10^4$	0.19544(136)	0.146967(668)	0.04221608	0.04220580
h_1	0.0 ^b	0.0 ^b	0.0 ^b	0.0 ^b
$h_2 \times 10^{13}$	0.0 ^b	0.0 ^b	0.139623	0.12838
$h_3 \times 10^{14}$	0.0 ^b	0.0 ^b	0.246250	0.21696
L_J	0.0 ^b	0.0 ^b	0.0 ^b	0.0 ^b
L_{JK}	0.0 ^b	0.0 ^b	0.0 ^b	0.0 ^b
L_{KJ}	0.0 ^b	0.0 ^b	0.0 ^b	0.0 ^b
$L_{KKJ} \times 10^9$	–0.7624(426)	0.0 ^b	–0.079240	–0.063049
$L_K \times 10^7$	–0.9444(195)	0.0 ^b	–0.0676427	–0.0684323
l_1	0.0 ^b	0.0 ^b	0.0 ^b	0.0 ^b
l_2	0.0 ^b	0.0 ^b	0.0 ^b	0.0 ^b
l_3	0.0 ^b	0.0 ^b	0.0 ^b	0.0 ^b
l_4	0.0 ^b	0.0 ^b	0.0 ^b	0.0 ^b
NFAD	2495/2661	1451/1491		
SDO	5.9×10^{-4}	6.9×10^{-4}		

^a Standard deviations in parentheses refer to the least significant digits.

^b Constrained.

parameters. Unfortunately, a truly revealing comparison is hindered by the different choice of the refined parameters for the two isotopologues.

A comparison between the $\nu_2 = 2$ and GS parameters in Table 6 reveals anomalous percentage differences between some of the parameters, both for $\text{H}^{16}\text{O}^{35}\text{Cl}$ and $\text{H}^{16}\text{O}^{37}\text{Cl}$; in particular, they are larger than 50% for d_2 , H , and L . These parameters should be considered as effective ones since they absorb the effects of rovibrational perturbations with closest vibrational states not considered explicitly in the analysis. Similar anomalies characterize the parameters of the $\nu_2 = 1$ state [17]. The analysis of this state revealed that the $K_a = 5$ levels of $\text{H}^{16}\text{O}^{35}\text{Cl}$ were perturbed by a Coriolis interaction with the $K_a = 4$ levels of $\nu_3 = 2$ and were excluded from the fit. The same interaction could be present between the same levels of $\nu_2 = 2$ and $\nu_2 = 1$ and $\nu_3 = 2$, also considering that the separation between the energies of the interacting vibrational states is practically the same, *i.e.*, about 200 cm^{-1} , see Table 4. This hypothesis is supported by the results of a fit of $\text{H}^{16}\text{O}^{35}\text{Cl}$ with L_{KKJ} and L_K constrained to their GS values. The total number of rejected transitions increases from 166 to 368, whereas the number of discarded transitions with $K'_a = 5$ is 246 instead of 38, mainly with $J \geq 10$. The exclusion of transitions with $K'_a = 5$ from the fit decreases the number of discarded lines from 166 to 111. The set of parameters in Table 6 can also be compared to those listed in Table 2 of Ref. [11]. A smaller number of parameters has been refined in the present analysis. For $\text{H}^{16}\text{O}^{37}\text{Cl}$, H_J and H_{JK} have been refined, whereas L_{KKJ} and L_K , as well as h_2 and h_3 for both molecules were fixed to zero. The values of the corresponding parameters are very similar, the percentage differences being about zero for B , D , and d_1 . Much larger differences are observed for H_J and H_{JK} as a consequence of the different choice of refined parameters. Overall, the parameters in Table 6 can be considered the preferred ones, notwithstanding the limits evidenced in the above discussion.

8. Comparison with the HITRAN line-by-line dataset

There have been no changes between HITRAN2016 [2] and HITRAN2020 [3] for HOCl, both datasets contain 8877 and 7399 transitions for $\text{H}^{16}\text{O}^{35}\text{Cl}$ and $\text{H}^{16}\text{O}^{37}\text{Cl}$, respectively, restricted to the 1–3800

cm^{-1} range. It is worth comparing the HITRAN and MARVEL datasets and check, in particular, the completeness of the MARVEL dataset containing only experimentally measured and assigned transitions. Furthermore, our first-principles line lists allow checking the completeness of the HITRAN dataset.

8.1. MARVEL data for $\text{H}^{16}\text{O}^{35}\text{Cl}$

The HITRAN2020 database of $\text{H}^{16}\text{O}^{35}\text{Cl}$ was constructed using the transitions and the spectroscopic parameters reported in 84SiAnDaGe [16], 98FIBiWaOr [25], and 00AuKIFIPa [26]. The MARVEL collection of experimental data has 10266 validated transitions, a significantly larger number than 8877. At the same time, our MARVEL treatment goes to much higher wavenumber values, up to 14566 cm^{-1} . Most importantly, a lot of the HITRAN2020 line positions are based on EH calculations, while the present dataset strictly contains measured data. After checking the correctness of the HITRAN energy-level entries, it was found that altogether 611 lines contain rotational labels for $\text{H}^{16}\text{O}^{35}\text{Cl}$ where the value of K_c is set to zero. This is due to a convention used in HITRAN: when the two K_c sublevels ($J, K_a, J - K_a$) and ($J, K_a, J - K_a + 1$) of a near prolate asymmetric top are degenerate, only one is listed, with K_c set to 0.

Since HITRAN utilizes EH results, it is not surprising that there are about 4000 lines in the 1170–3800 cm^{-1} region that are not available in our experimental database. As found in this study, the accuracy of some of these EH-based lines can be questioned, especially those which involve upper state energies extrapolated from EH values. Our MARVEL database contains about 3500 extra lines which are not part of the HITRAN dataset. Surprisingly, some of these extra lines are in the microwave (MW) region (for example, $(000)[101] \leftarrow (000)[000]$ or $(000)[211] \leftarrow (000)[110]$). It is also important to emphasize that all other HITRAN lines can be reproduced by the empirical (MARVEL) energy levels of this study within 0.009 cm^{-1} , attesting the general accuracy of the EH models developed for HOCl.

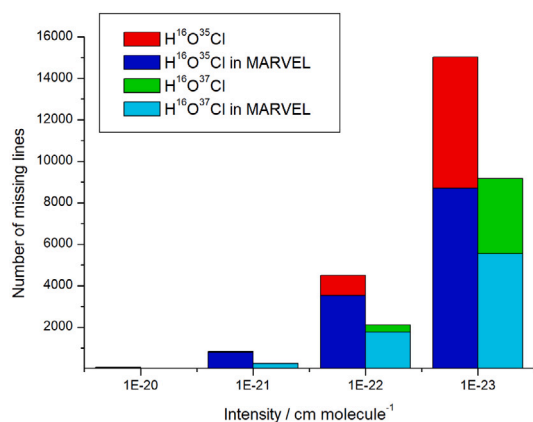


Fig. 7. The number of missing HITRAN lines for H¹⁶O³⁵Cl and H¹⁶O³⁷Cl as a function of intensity.

8.2. MARVEL data for H¹⁶O³⁷Cl

Similar to the case of H¹⁶O³⁵Cl, the H¹⁶O³⁷Cl HITRAN dataset was also constructed using the transitions and spectroscopic parameters reported in 84SiAnDaGe [16], 98FIBiWaOr [25], and 00AuKIFlPa [26]. This HITRAN database contains 456 lines with rotational labels where $K_c = 0$ and about 4000 rovibrational lines in the 1170–3800 cm⁻¹ region that are not available in our experimental database. It is also true that our database contains more than 2000 extra lines up to 3800 cm⁻¹ which are not part of the HITRAN dataset.

8.3. First-principles line lists

In the 0–3000 cm⁻¹ region, the first-principles line lists of H¹⁶O³⁵Cl and H¹⁶O³⁷Cl contain 5 136 239 and 4 346 046 rovibrational transitions, respectively, while $J_{\max} = 45$. As Fig. 7 shows, there are a lot of transitions missing in HITRAN even when the intensity is large. It can be seen in Fig. 7 that while the number of missing lines is large, about half of them are predicted by the accurate empirical (MARVEL) energy levels, making their eventual detection particularly straightforward.

9. Summary and conclusions

During the search of the literature for measured and assigned high-resolution rovibrational transitions of hypochlorous acid and the analysis of the spectroscopic data, minor issues were found with our MARVEL analysis, published in Ref. [1], for the H¹⁶O³⁵Cl transitions. Even more importantly, it became possible to include the originally measured transitions of Ref. [26] into our transitions list, replacing the originally considered effective-Hamiltonian values. Consequently, as part of this study, we updated the MARVEL analysis of H¹⁶O³⁵Cl. The improved set of transitions and empirical energy levels can be found in the Supplementary Material to this paper.

As a next step, all experimentally measured and assigned rovibrational transitions of the H¹⁶O³⁷Cl isotopologue of hypochlorous acid have been collated into a database and the transitions were analysed using the MARVEL protocol. The current MARVEL database contains experimentally measured transitions from three older sources [11,20,26]; these transitions were not reported explicitly in the original publications. The MARVEL database contains more than 10 000 experimental transitions collected from 16 sources, most of which could be validated. Using these transitions we determined close to 4000 empirical rovibrational energy levels on the ground electronic state, corresponding to 13 vibrational parent states.

It is worth noting that while 10 VBO values are known experimentally for the parent H¹⁶O³⁵Cl isotopologue, only three (and only one

below 7000 cm⁻¹) have been measured experimentally for H¹⁶O³⁷Cl (not counting the ground vibrational state). The empirical rovibrational energies of H¹⁶O³⁵Cl and H¹⁶O³⁷Cl have been checked against effective Hamiltonian values as well as results from extensive variational nuclear-motion computations, utilizing an exact kinetic-energy operator and an empirically adjusted potential energy surface. The empirical energy sets of the two isotopologues have also been checked against each other, ensuring their complete consistency.

Since the high-resolution spectrum between 2300 and 2800 cm⁻¹ (the $2\nu_2$ band region), recorded as part of the study reported in Ref. [11], remained available electronically, a search was executed, based on the empirical (MARVEL) energies, looking for further assignable transitions. This search resulted in a large number of newly assigned transitions but very few new empirical energy levels. The newly assigned experimental transitions are part of the MARVEL input and output files, given as Supplementary Material, with the tag ‘23EcSiFuRa’. The availability of new transitions made possible an improved estimate of a large number of effective Hamiltonian parameters for the $2\nu_2$ state.

Based on potential-energy and dipole-moment surfaces taken from the literature, first-principles line lists were generated for H¹⁶O³⁵Cl and H¹⁶O³⁷Cl. The lists of the computed energy levels, upon which the line lists are based, are complete up to 3000 cm⁻¹ and up to $J_{\max} = 45$. These computed line lists reveal a significant number of missing high-intensity lines in the canonical spectroscopic line-by-line database HITRAN [2,3]. It is desirable to design experiments yielding at least these transitions in the region covered by HITRAN. Comparisons with the HOCl entries of HITRAN also reveal that the present datasets, containing experimentally measured transitions and not results from effective-Hamiltonian fits, are significantly more complete in their wavenumber coverage.

Declaration of competing interest

The authors declare that they have no known competing financial interests or personal relationships that could have appeared to influence the work reported in this paper.

Acknowledgements

The work performed in Budapest received support from NKFIH (grant no. K138233). The authors would like to express their gratitude to Prof. Jean Vander Auwera for providing the measured data of Ref. [26] and for useful discussions. Conversations with Dr. Csaba Fábri on aspects of variational nuclear-motion computations are gratefully acknowledged. This publication supports research performed within the COST Action CA21101 “Confined molecular systems: from a new generation of materials to the stars” (COSY), funded by the European Cooperation in Science and Technology (COST) and the MSCA Doctoral Network PHYMOL: “Physics, accuracy and machine learning, towards the next generation of molecular potentials”.

Appendix A. Supplementary data

Supplementary material related to this article can be found online at <https://doi.org/10.1016/j.jms.2023.111834>.

References

- [1] B. Rácsai, T. Furtenbacher, L. Fusina, G. Di Lonardo, A.G. Császár, MARVEL analysis of the high-resolution rovibrational spectra of H¹⁶O³⁵Cl, *J. Mol. Spectrosc.* 384 (2022) 111561, <http://dx.doi.org/10.1016/j.jms.2021.111561>.
- [2] I.E. Gordon, L.S. Rothman, C. Hill, R.V. Kochanov, Y. Tan, P.F. Bernath, M. Birk, V. Boudon, A. Campargue, K.V. Chance, B.J. Drouin, J.-M. Flaud, R.R. Gamache, J.T. Hodges, D. Jacquemart, V.I. Perevalov, A. Perrin, K.P. Shine, M.-A.H. Smith, J. Tennyson, G.C. Toon, H. Tran, V.G. Tyuterev, A. Barbe, A.G. Császár, V.M. Devi, T. Furtenbacher, J.J. Harrison, J.-M. Hartmann, A. Jolly, T.J. Johnson, T. Karman, I. Kleiner, A.A. Kyuberis, J. Loos, O.M. Lyulin, S.T. Massie, S.N. Mikhailenko, N. Moazzen-Ahmadi, H.S.P. Müller, O.V. Naumenko, A.V. Nikitin,

- O.L. Polyansky, M. Rey, M. Rotger, S.W. Sharpe, K. Sung, E. Starikova, S.A. Tashkun, J. Vander Auwera, G. Wagner, J. Wilzewski, P. Wcislo, S. Yu, E.J. Zak, The HITRAN2016 molecular spectroscopic database, *J. Quant. Spectrosc. Radiat. Transfer* 203 (2017) 3–69, <http://dx.doi.org/10.1016/j.jqsrt.2017.06.038>.
- [3] I.E. Gordon, L.S. Rothman, R.J. Hargreaves, R. Hashemi, E.V. Karlovets, F.M. Skinner, E.K. Conway, C. Hill, R.V. Kochanov, Y. Tan, P. Wcislo, A.A. Finenko, K. Nelson, P.F. Bernath, M. Birk, V. Boudon, A. Campargue, K.V. Chance, A. Coustenis, B.J. Drouin, J. Flaud, R.R. Gamache, J.T. Hodges, D. Jacquemart, E.J. Mlawer, A.V. Nikitin, V.I. Perevalov, M. Rotger, J. Tennyson, G.C. Toon, H. Tran, V.G. Tyuterev, E.M. Adkins, A. Baker, A. Barbe, E. Canè, A.G. Császár, A. Dudaryonok, O. Egorov, A.J. Fleisher, H. Fleurbaey, A. Foltynowicz, T. Furtenbacher, J.J. Harrison, J. Hartmann, V. Horneman, X. Huang, T. Karman, J. Karns, S. Kassi, I. Kleiner, V. Kofman, F. Kwabia-Tchana, N.N. Lavrentieva, T.J. Lee, D.A. Long, A.A. Lukashchuk, O.M. Lyulin, V.Y. Makhnev, W. Matt, S.T. Massie, M. Melosso, S.N. Mikhailenko, D. Mondelain, H.S.P. Müller, O. Naumenko, A. Perrin, O.L. Polyansky, E. Raddaoui, P.L. Raston, Z.D. Reed, M. Rey, C. Richard, R. Tóbiás, I. Sadiek, D.W. Schwenke, E. Starikova, K. Sung, F. Tamassia, S.A. Tashkun, J. Vander Auwera, I.A. Vasilenko, A.A. Viganin, G.L. Villanueva, B. Vispoel, G. Wagner, A. Yachmenev, S.N. Yurchenko, The HITRAN2020 molecular spectroscopic database, *J. Quant. Spectrosc. Radiat. Transfer* 277 (2022) 107949, <http://dx.doi.org/10.1016/j.jqsrt.2021.107949>.
- [4] T. Furtenbacher, A.G. Császár, J. Tennyson, MARVEL: measured active rotational-vibrational energy levels, *J. Mol. Spectrosc.* 245 (2007) 115–125, <http://dx.doi.org/10.1016/j.jms.2007.07.005>.
- [5] T. Furtenbacher, A.G. Császár, MARVEL: measured active rotational-vibrational energy levels. II. Algorithmic improvements, *J. Quant. Spectrosc. Radiat. Transfer* 113 (2012) 929–935, <http://dx.doi.org/10.1016/j.jqsrt.2012.01.005>.
- [6] T. Furtenbacher, A.G. Császár, The role of intensities in determining characteristics of spectroscopic networks, *J. Mol. Spectrosc.* 1009 (2012) 123–129, <http://dx.doi.org/10.1016/j.molstruc.2011.10.057>.
- [7] R. Tóbiás, T. Furtenbacher, J. Tennyson, A.G. Császár, Accurate empirical rovibrational energies and transitions of H_2^{16}O , *Phys. Chem. Chem. Phys.* 21 (2019) 3473–3495, <http://dx.doi.org/10.1039/C8CP05169K>.
- [8] A.G. Császár, T. Furtenbacher, Spectroscopic networks, *J. Mol. Spectrosc.* 266 (2011) 99–103, <http://dx.doi.org/10.1016/j.jms.2011.03.031>.
- [9] T. Furtenbacher, P. Árendás, G. Mellau, A.G. Császár, Simple molecules as complex systems, *Sci. Rep.* 4 (2014) 4654, <http://dx.doi.org/10.1038/srep04654>.
- [10] A.G. Császár, T. Furtenbacher, P. Árendás, Small molecules – big data, *J. Phys. Chem. A* 120 (2016) 8949–8969, <http://dx.doi.org/10.1021/acs.jpca.6b02293>.
- [11] F. Cavazza, G. Di Lonardo, L. Fusina, The $2\nu_2$ band of HOCl, *Gazz. Chim. Ital.* 126 (1996) 539–541.
- [12] D.C. Lindsey, D.G. Lister, D.J. Millen, The microwave spectrum and structure of hypochlorous acid, *J. Chem. Soc. D: Chem. Commun.* (1969) 950–951, <http://dx.doi.org/10.1039/C29690000950>.
- [13] A.M. Mirri, F. Scappini, G. Cazzoli, Microwave spectrum, structure and electric quadrupole coupling constants of HOCl, *J. Mol. Spectrosc.* 38 (1971) 218–227, [http://dx.doi.org/10.1016/0022-2852\(71\)90107-x](http://dx.doi.org/10.1016/0022-2852(71)90107-x).
- [14] J.S. Wells, R.L. Sams, W.J. Lafferty, The high resolution infrared spectrum of the ν_1 band of HOCl, *J. Mol. Spectrosc.* 77 (1979) 349–364, [http://dx.doi.org/10.1016/0022-2852\(79\)90177-2](http://dx.doi.org/10.1016/0022-2852(79)90177-2).
- [15] R.L. Sams, W.B. Olson, Analysis of the high-resolution infrared spectrum of the ν_2 bending mode of HOCl at 1238 cm^{-1} , *J. Mol. Spectrosc.* 84 (1980) 113–123, [http://dx.doi.org/10.1016/0022-2852\(80\)90244-1](http://dx.doi.org/10.1016/0022-2852(80)90244-1).
- [16] H.E. Gillis Singbeil, W.D. Anderson, R.W. Davis, M.C.L. Gerry, E.A. Cohen, H.M. Pickett, F.J. Lovas, R.D. Suenram, The microwave and millimeter-wave spectra of hypochlorous acid, *J. Mol. Spectrosc.* 103 (1984) 466–485, [http://dx.doi.org/10.1016/0022-2852\(84\)90069-9](http://dx.doi.org/10.1016/0022-2852(84)90069-9).
- [17] W.J. Lafferty, W.B. Olson, The high-resolution infrared spectra of the ν_2 and ν_3 bands of HOCl, *J. Mol. Spectrosc.* 120 (1986) 359–373, [http://dx.doi.org/10.1016/0022-2852\(86\)90010-x](http://dx.doi.org/10.1016/0022-2852(86)90010-x).
- [18] M. Carlotti, G. Di Lonardo, L. Fusina, A. Trombetti, B. Carli, The far-infrared spectrum of hypochlorous acid, HOCl, *J. Mol. Spectrosc.* 141 (1990) 29–42, [http://dx.doi.org/10.1016/0022-2852\(90\)90275-u](http://dx.doi.org/10.1016/0022-2852(90)90275-u).
- [19] F. Cavazza, G. Di Lonardo, R. Escibano, L. Fusina, P.C. Gomez, J. Ortigoso, The $2\nu_1$ band of HOCl, *J. Mol. Spectrosc.* 159 (1993) 395–409, <http://dx.doi.org/10.1006/jmsp.1993.1137>.
- [20] C. Azzolini, F. Cavazza, G. Crovetto, G. Di Lonardo, R. Frulla, R. Escibano, L. Fusina, Infrared spectroscopy of HOCl in the $4000\text{--}10\,000\text{ cm}^{-1}$ region, *J. Mol. Spectrosc.* 168 (1994) 494–506, <http://dx.doi.org/10.1006/jmsp.1994.1296>.
- [21] M. Bellini, P. De Natale, L. Fusina, G. Modugno, The pure rotation spectrum of HOCl in the submillimeter-wave region, *J. Mol. Spectrosc.* 172 (1995) 559–562, <http://dx.doi.org/10.1006/jmsp.1995.1202>.
- [22] B. Abel, H.H. Hamann, A.A. Kachanov, J. Troe, Intracavity laser absorption spectroscopy of HOCl overtones. I. The $3\nu_1+2\nu_2$ band and numbers of vibrational states, *J. Chem. Phys.* 104 (1996) 3189–3197, <http://dx.doi.org/10.1063/1.471016>.
- [23] A. Charvát, S.F. Deppe, H.H. Hamann, B. Abel, The $3\nu_1+\nu_2$ combination band of HOCl: Assignments, perturbations, and line intensities, *J. Mol. Spectrosc.* 185 (1997) 336–346, <http://dx.doi.org/10.1006/jmsp.1997.7382>.
- [24] H.H. Hamann, A. Charvát, B. Abel, S.A. Kovalenko, A.A. Kachanov, Intracavity laser absorption spectroscopy of HOCl. II. High overtones, perturbations, and intramolecular dynamics, *J. Chem. Phys.* 106 (1997) 3103–3116, <http://dx.doi.org/10.1063/1.473053>.
- [25] J.-M. Flaud, M. Birk, G. Wagner, J. Orphal, S. Klee, W. Lafferty, The far infrared spectrum of HOCl: Line positions and intensities, *J. Mol. Spectrosc.* 191 (1998) 362–367, <http://dx.doi.org/10.1006/jmsp.1998.7653>.
- [26] J. Vander Auwera, J. Kleffmann, J.-M. Flaud, G. Pawelke, H. Bürger, D. Hurtmans, R. Pétrisse, Absolute ν_2 line intensities of HOCl by simultaneous measurements in the infrared with a tunable diode laser and far-infrared region using a Fourier transform spectrometer, *J. Mol. Spectrosc.* 204 (2000) 36–47, <http://dx.doi.org/10.1006/jmsp.2000.8197>.
- [27] J.H. Shorter, D.D. Nelson, M.S. Zahniser, Air-broadened linewidth measurements in the ν_2 vibrational band of HOCl, *J. Chem. Soc. Farad. Trans.* 93 (1997) 2933–2935, <http://dx.doi.org/10.1039/a701984j>.
- [28] I.E. Gordon, M.R. Potterbusch, D. Bouquin, C.C. Erdmann, J.S. Wilzewski, L.S. Rothman, Are your spectroscopic data being used? *J. Mol. Spectrosc.* 327 (2016) 232–238, <http://dx.doi.org/10.1016/j.jms.2016.03.011>.
- [29] R.S. Mulliken, Report on notation for the spectra of polyatomic molecules, *J. Chem. Phys.* 23 (1955) 1997–2011, <http://dx.doi.org/10.1063/1.1740655>.
- [30] R. Zare, *Angular Momentum: Understanding Spatial Aspects in Chemistry and Physics*, Wiley, New York, 1988.
- [31] H. Kroto, *Molecular Rotation Spectra*, Dover, New York, 1992.
- [32] P. Árendás, T. Furtenbacher, A.G. Császár, Selecting lines for spectroscopic (re)measurements to improve the accuracy of absolute energies of rovibronic quantum states, *J. Cheminform.* 13 (2021) 1, <http://dx.doi.org/10.1186/s13321-021-00534-y>.
- [33] S. Skokov, K.A. Peterson, J.M. Bowman, An accurate *ab initio* HOCl potential energy surface, vibrational and rotational calculations, and comparison with experiment, *J. Chem. Phys.* 109 (1998) 2662–2671, <http://dx.doi.org/10.1063/1.476865>.
- [34] P. Botschwina, Vibrational frequencies from anharmonic *ab initio*/empirical potential energy functions: I. method and application to H_2O , HNO, HOF and HOCl, *Chem. Phys.* 40 (1979) 33–44, [http://dx.doi.org/10.1016/0301-0104\(79\)85116-2](http://dx.doi.org/10.1016/0301-0104(79)85116-2).
- [35] A. Komornicki, R.L. Jaffe, An *ab initio* investigation of the structure, vibrational frequencies, and intensities of HO_2 and HOCl, *J. Chem. Phys.* 71 (1979) 2150–2155, <http://dx.doi.org/10.1063/1.438588>.
- [36] J.N. Murrell, S. Carter, I.M. Mills, M.F. Guest, Analytical potentials for triatomic molecules from spectroscopic data. V. Application to HOX (X=F, Cl, Br, I), *Mol. Phys.* 37 (1979) 1199–1222, <http://dx.doi.org/10.1080/00268977900100881>.
- [37] L. Halonen, T.K. Ha, *Ab initio* calculation and anharmonic force field of hypochlorous acid, HOCl, *J. Chem. Phys.* 88 (1988) 3775–3779, <http://dx.doi.org/10.1063/1.454728>.
- [38] R. Escibano, G. Di Lonardo, L. Fusina, Empirical anharmonic force field and equilibrium structure of hypochlorous acid, HOCl, *Chem. Phys. Lett.* 259 (1996) 614–618, [http://dx.doi.org/10.1016/0009-2614\(96\)00774-9](http://dx.doi.org/10.1016/0009-2614(96)00774-9).
- [39] S. Skokov, J. Qi, J.M. Bowman, C.-Y. Yang, S.K. Gray, K.A. Peterson, V.A. Mandelshtam, Accurate variational calculations and analysis of the HOCl vibrational energy spectrum, *J. Chem. Phys.* 109 (1998) 10273–10283, <http://dx.doi.org/10.1063/1.477723>.
- [40] J. Hauschildt, J. Weiss, C. Beck, S.Y. Grebenshchikov, R. Dören, R. Schinke, J. Koput, Unimolecular dissociation of HOCl: unexpectedly broad distribution of rate constants, *Chem. Phys. Lett.* 300 (1999) 569–576, [http://dx.doi.org/10.1016/S0009-2614\(98\)01432-8](http://dx.doi.org/10.1016/S0009-2614(98)01432-8).
- [41] R. Jost, M. Joyeux, S. Skokov, J.M. Bowman, Vibrational analysis of HOCl up to 98% of the dissociation energy with a Fermi resonance Hamiltonian, *J. Chem. Phys.* 111 (1999) 6807–6820, <http://dx.doi.org/10.1063/1.479974>.
- [42] K. Aarset, A.G. Császár, E. Sibert, W.D. Allen, H.F. Schaefer III, W. Klopper, J. Noga, Anharmonic force field, vibrational energy levels, and barrier to inversion of SiH_3^- , *J. Chem. Phys.* 112 (2000) 4053–4063, <http://dx.doi.org/10.1063/1.481596>.
- [43] K.A. Peterson, S. Skokov, J.M. Bowman, A theoretical study of the vibrational energy spectrum of the HOCl/HClO system on an accurate *ab initio* potential energy surface, *J. Chem. Phys.* 111 (1999) 7446–7456, <http://dx.doi.org/10.1063/1.480069>.
- [44] S. Skokov, K.A. Peterson, J.M. Bowman, Perturbative inversion of the HOCl potential energy surface via singular value decomposition, *Chem. Phys. Lett.* 191 (1999) 362–367, [http://dx.doi.org/10.1016/S0009-2614\(99\)00996-3](http://dx.doi.org/10.1016/S0009-2614(99)00996-3).
- [45] M. Joyeux, D. Sugny, M. Lombardi, R. Jost, R. Schinke, S. Skokov, J. Bowman, Vibrational dynamics up to the dissociation threshold: A case study of two-dimensional HOCl, *J. Chem. Phys.* 113 (2000) 9610–9621, <http://dx.doi.org/10.1063/1.1321031>.
- [46] J. Weiß, J. Hauschildt, S.Y. Grebenshchikov, R. Dören, R. Schinke, J. Koput, S. Stamatiadis, S.C. Farantos, Saddle-node bifurcations in the spectrum of HOCl, *J. Chem. Phys.* 112 (2000) 77–93, <http://dx.doi.org/10.1063/1.480563>.
- [47] H.Y. Mussa, J. Tennyson, Calculating quasi-bound rotation-vibrational states of HOCl using massively parallel computers, *Chem. Phys. Lett.* 366 (2002) 449–457, [http://dx.doi.org/10.1016/S0009-2614\(02\)01554-3](http://dx.doi.org/10.1016/S0009-2614(02)01554-3).

- [48] S. Nanbu, M. Aoyagi, H. Kamisaka, H. Nakamura, W. Bian, K. Tanaka, Chemical reaction in the $O(^1D) + HCl$ system I. Ab initio global potential energy surfaces for the $1^1A'$, $2^1A'$, and $1^1A''$ states, *J. Theor. Comput. Chem.* 1 (2002) 263, <http://dx.doi.org/10.1142/S0219633602000191>.
- [49] H. Zhang, S.C. Smith, S. Nanbu, H. Nakamura, HOCl ro-vibrational bound-state calculations for nonzero total angular momentum, *J. Phys. Chem. A* 110 (2006) 5468–5474, <http://dx.doi.org/10.1021/jp058286n>.
- [50] Y.-D. Lin, L.E. Reichl, C. Jung, The vibrational dynamics of 3D HOCl above dissociation, *J. Chem. Phys.* 142 (2015) 124304, <http://dx.doi.org/10.1063/1.4915142>.
- [51] E.B. Wilson Jr., J.C. Decius, P.C. Cross, *Molecular Vibrations: The Theory of Infrared and Raman Vibrational Spectra*, McGraw Hill, New York, 1955.
- [52] H. Nielsen, The vibration-rotation energies of molecules, *Rev. Modern Phys.* 23 (1951) 90–136, <http://dx.doi.org/10.1103/revmodphys.23.90>.
- [53] D.A. Clabo, W.D. Allen, R.B. Remington, Y. Yamaguchi, H.F. Schaefer III, A systematic study of molecular vibrational anharmonicity and vibration-rotation interaction by self-consistent-field higher derivative methods. asymmetric top molecules, *Chem. Phys.* 123 (1988) 187–239, [http://dx.doi.org/10.1016/0301-0104\(88\)87271-9](http://dx.doi.org/10.1016/0301-0104(88)87271-9).
- [54] W.D. Allen, Y. Yamaguchi, A.G. Császár, D.A. Clabo Jr., R.B. Remington, H.F. Schaefer III, A systematic study of molecular vibrational anharmonicity and vibration-rotation interaction by self-consistent-field higher derivative methods. Linear polyatomic molecules, *Chem. Phys.* 145 (1990) 427–466, [http://dx.doi.org/10.1016/0301-0104\(90\)87051-C](http://dx.doi.org/10.1016/0301-0104(90)87051-C).
- [55] T.H. Dunning Jr., Gaussian basis sets for use in correlated molecular calculations. I. The atoms boron through neon and hydrogen, *J. Chem. Phys.* 90 (1989) 1007–1023, <http://dx.doi.org/10.1063/1.456153>.
- [56] K. Raghavachari, G.W. Trucks, J.A. Pople, M. Head-Gordon, A fifth-order perturbation comparison of electron correlation theories, *Chem. Phys. Lett.* 157 (1989) 479–483, [http://dx.doi.org/10.1016/S0009-2614\(89\)87395-6](http://dx.doi.org/10.1016/S0009-2614(89)87395-6).
- [57] A.G. Császár, C. Fábri, T. Szidarovszky, E. Mátyus, T. Furtenbacher, G. Czakó, The fourth age of quantum chemistry: molecules in motion, *Phys. Chem. Chem. Phys.* 14 (2012) 1085–1106, <http://dx.doi.org/10.1039/C1CP21830A>.
- [58] E. Mátyus, G. Czakó, A.G. Császár, Toward black-box-type full- and reduced-dimensional variational (ro)vibrational computations, *J. Chem. Phys.* 130 (2009) 134112, <http://dx.doi.org/10.1063/1.3076742>.
- [59] C. Fábri, E. Mátyus, A.G. Császár, Rotating full- and reduced-dimensional quantum chemical models of molecules, *J. Chem. Phys.* 134 (2011) 074105, <http://dx.doi.org/10.1063/1.3533950>.
- [60] C. Fábri, M. Quack, A.G. Császár, On the use of nonrigid-molecular symmetry in nuclear-motion computations employing a discrete variable representation: a case study of the bending energy levels of CH_3^+ , *J. Chem. Phys.* 147 (2017) 134101, <http://dx.doi.org/10.1063/1.4990297>.
- [61] D.O. Harris, G.G. Engerholm, W.D. Gwinn, Calculation of matrix elements for one-dimensional quantum-mechanical problems and the application to anharmonic oscillators, *J. Chem. Phys.* 43 (1965) 1515–1517, <http://dx.doi.org/10.1063/1.1696963>.
- [62] J.C. Light, T. Carrington, Discrete variable representations and their utilization, *Adv. Chem. Phys.* 114 (2000) 263–310, <http://dx.doi.org/10.1002/9780470141731.ch4>.
- [63] K.A. Peterson, Accurate ab initio near-equilibrium potential energy and dipole moment functions of HOCl and HOBr, *Spectrochim. Acta A* 53 (1997) 1051–1064, [http://dx.doi.org/10.1016/S1386-1425\(97\)00014-0](http://dx.doi.org/10.1016/S1386-1425(97)00014-0).
- [64] E. Mátyus, C. Fábri, T. Szidarovszky, G. Czakó, W.D. Allen, A.G. Császár, Assigning quantum labels to variationally computed rotational-vibrational eigenstates of polyatomic molecules, *J. Chem. Phys.* 133 (2010) 034113, <http://dx.doi.org/10.1063/1.3451075>.
- [65] T. Szidarovszky, C. Fábri, A.G. Császár, The role of axis embedding on rigid rotor decomposition analysis of variational rovibrational wave functions, *J. Chem. Phys.* 136 (2012) 174112, <http://dx.doi.org/10.1063/1.4707463>.
- [66] J.D. Louck, H.W. Galbraith, Eckart vectors, eckart frames, and polyatomic molecules, *Rev. Modern Phys.* 48 (1976) 69–106, <http://dx.doi.org/10.1103/RevModPhys.48.69>.
- [67] C. Fábri, E. Mátyus, A.G. Császár, Numerically constructed internal-coordinate Hamiltonian with Eckart embedding and its application for the inversion tunneling of ammonia, *Spectrochim. Acta A* 119 (2014) 84–89, <http://dx.doi.org/10.1016/j.saa.2013.03.090>.
- [68] J. Pesonen, Eckart frame vibration-rotation Hamiltonians: Contravariant metric tensor, *J. Chem. Phys.* 140 (2014) 074101, <http://dx.doi.org/10.1063/1.4865750>.
- [69] A. Al-Derzi, J. Tennyson, S. Yurchenko, M. Melosso, N. Jiang, C. Puzzarini, L. Dore, T. Furtenbacher, R. Tóbiás, A.G. Császár, An improved rovibrational line list of formaldehyde, $H_2^{12}C^{16}O$, *J. Quant. Spectrosc. Radiat. Transfer* 266 (2021) 107563, <http://dx.doi.org/10.1016/j.jqsrt.2021.107563>.
- [70] A.R. Al Derzi, T. Furtenbacher, S.N. Yurchenko, J. Tennyson, A.G. Császár, MARVEL analysis of the measured high-resolution spectra of $^{14}NH_3$, *J. Quant. Spectrosc. Radiat. Transfer* 161 (2015) 117–130, <http://dx.doi.org/10.1016/j.jqsrt.2015.03.034>.
- [71] T. Furtenbacher, P.A. Coles, J. Tennyson, S.N. Yurchenko, S. Yu, B. Drouin, R. Tóbiás, A.G. Császár, Empirical rovibrational energy levels of ammonia up to 7500 cm^{-1} , *J. Quant. Spectrosc. Radiat. Transfer* 251 (2020) 107027, <http://dx.doi.org/10.1016/j.jqsrt.2020.107027>.
- [72] C. Fábri, E. Mátyus, T. Furtenbacher, L. Nemes, B. Mihály, T. Zoltáni, A.G. Császár, Variational quantum mechanical and active database approaches to the rotational-vibrational spectroscopy of ketene, H_2CCO , *J. Chem. Phys.* 135 (2011) 094307, <http://dx.doi.org/10.1063/1.3625404>.
- [73] M.L. Junttila, W.J. Lafferty, J.B. Burkholder, The high-resolution spectrum of the ν_1 band and ground state rotational constants of HOCl, *J. Mol. Spectrosc.* 164 (1994) 583–585, <http://dx.doi.org/10.1006/jmsp.1994.1102>.
- [74] J.K.G. Watson, Aspects of quartic and sextic centrifugal effects on rotational energy levels, in: J. Durig (Ed.), *Vibrational Spectra and Structure*, Vol. 6, Elsevier, Amsterdam, 1977.